Boundary-Layer Meteorology manuscript No.
(will be inserted by the editor)

Exact analytic solution for slope flows with spatially varying eddy viscosity and diffusivity

M. G. Giometto · R. Grandi · J. Fang · M.B. Parlange

Received: DD Month YEAR / Accepted: DD Month YEAR

Abstract An exact analytic solution of the steady-state Prandtl model equations is derived, valid for spatially varying eddy diffusivities (O'Briens type) and Prandtl number of unity. In this formulation profiles show significant variations in both phase and amplitude of minima-maxima with respect to the classic constant eddy viscosity model and the more recent, approximate, WKB solution. The near wall region is characterized by a relatively stronger surface inversion and velocity gradients, the low-level-jet is further displaced toward the wall, and its peak velocity strongly depends on the model parameter, suggesting a tighter coupling between dynamics and thermodynamics.

1 Introduction

Natural convection of turbulent stratified flows over sloping surfaces is ubiquitous in nature and engineering, and is of interest not only as a fundamental problem in itself, but also because of the important role it plays over a broad

M.G. Giometto
School of Architecture, Civil and Environmental Engineering, École Polytechnique Fédérale de Lausanne, Lausanne, Switzerland
E-mail: marco.giometto@epfl.ch

Riccardo Grandi
Mathematics Institute for Geometry and Applications, École Polytechnique Fédérale de Lausanne, Lausanne, Switzerland

J. Fang
School of Architecture, Civil and Environmental Engineering, École Polytechnique Fédérale de Lausanne, Lausanne, Switzerland

M.B. Parlange
Civil Engineering, Faculty of Applied Sciences, University of British Columbia, Vancouver, BC, Canada

range of scales and applications. On a local scale, for instance, it governs local weather conditions, affecting atmospheric transport processes and dispersion of scalars such as heat and humidity (Monti et al., 2002; Nylen et al., 2004). On a regional scale, it drives the development of deep-convective circulations (Egger, 1985; Parish and Bromwich, 1998) and is responsible for intense cyclonic vorticity in the middle and upper troposphere (Parish, 1992). Further, recent experimental field campaigns (Chu, 1987; Oerlemans and Vugts, 1993) have shown that persistent katabatic winds characterize the atmospheric boundary layer over snow-ice surfaces and glaciers, and therefore an accurate characterization of such flows is an essential component of understanding and modeling of the weather and climate. However, the complex dynamics (e.g. occurrence of intermittency, waves, Kelvin-Helmholtz instabilities and low-level jets) and the lack of a satisfactory similarity theory for such flows (Nadeau et al., 2013) pose a heavy burden in terms of computational requirements for numerical modellers; in most cases the required resolution is prohibitively costly (Fedorovich and Shapiro, 2009b,a; Spalart et al., 2011). Because of this, conceptual models are still of great interest, and represent a valid tool for the characterization of such systems. A cornerstone in the understanding of natural convection of stratified fluid along a sloping surface is represented by the classic Prandtl analytic model (Prandtl, 1942), and its more recent extensions/generalizations to include the effects of Coriolis force (Gutman and Malbakhov, 1964), external winds (Lykosov and Gutman, 1972), surface heterogeneity (Shapiro and Fedorovich, 2007; Oldroyd et al., 2014). The Prandtl model approximates the atmosphere in a Boussinesq sense and describes a steady flow over a thermally perturbed unbounded planar sloping surface that lies within a stratified environment, given by the following system of equations:

$$N^2 u(z) \sin\alpha = d(K_H db/dz)/dz, \tag{1}$$

$$b(z) \sin\alpha = -d(K_M du/dz)/dz, \tag{2}$$

where z denotes the normal-to-slope coordinate directions, u is the downslope velocity, b is buoyancy, N is the buoyancy frequency characterizing the system (related to the background stratification), α is the slope angle and K_M and K_H denote the eddy viscosity and diffusivity (an eddy viscosity/diffusivity model has been used to parametrize turbulent fluxes of momentum and buoyancy). Equations are defined in $z \in [z_0, \infty)$ with boundary conditions $u(z_0) = 0$, $u(z \to \infty) = 0$, $b(z_0) = b_s$ and $b(z \to \infty) = 0$ ($b_s > 0$ for upslope flows, whereas $b_s < 0$ for downslope flows).

The flow is assumed to be invariant in the downslope direction and the model can be used to determine its vertical structure. Eqs. 1 and 2 state that downslope (upslope) convection of cold (warm) air is balanced by momentum flux divergence, and that along-slope generated buoyancy is balanced by buoyancy flux divergence; thus the model is applicable away from ridges and valleys, so that advection terms are negligible (Nappo and Shankar, 1987). The Prandtl constant-K model is known to be overdissipative in the near surface regions, and therefore not able to represent the observed strong surface

gradients of temperature and momentum that commonly characterize katabatic and anabatic flows (Oerlemans, 1998; Grisogono and Oerlemans, 2001). Simple variations in the eddy diffusivity profiles were introduced in a matched analytic solution by Gutman (1983), and more recently Grisogono and Oerlemans (2001) considered general variations in the vertical structure of the eddy diffusivities, and derived solutions based on the WKB approximation (Bender and Orszag, 1999). The WKB solution is able to account for additional dynamics while still retaining an elegant form. However, that theory is only applicable when the model parameters (K_M, K_H) vary more slowly than the solution (u, b), and the validity of such a constraint for slope flows has been the subject of great debate (Grisogono and Oerlemans, 2002). In the following, we derive a closed-form solution to the Prandtl-model equations, valid for eddy viscosity / diffusivity coefficients that are modelled as a limited range of cubic polynomials, similar to what proposed in O'Brien (1970) for the planetary boundary layer. The solution thus represents an exact alternative to the WKB formulation for the chosen form of the model parameter. The new solution, expressed as a combination of Gaussian hypergeometric functions, is found to significantly differ from its analytical counterparts, shedding new light on the problem, and suggesting a different coupling between the dynamic and the thermodynamic boundary layers.

2 The Analytic Solution

We consider the one-dimensional Prandtl model (Eq. 1 and 2).

Assuming eddy diffusivities in line with the classic O'Brien's type (O'Brien, 1970), viz. $K(z) = Az(z-\zeta)^2$, where $\zeta > H$, $Pr = 1$ (i.e. $K_M = K_H = K$) and assigning a length, velocity and buoyancy scale $L = (N \sin\alpha)/A$, $U = b_s N^{-1}$ and $B = b_s$ respectively, Eqs. 1 and 2 reduce to:

$$\overline{u} = d(\overline{K} d\overline{b}/d\overline{z})/d\overline{z}, \qquad \text{in } [z_0, \overline{H}] \tag{3a}$$

$$\overline{b} = -d(\overline{K} d\overline{u}/d\overline{z})/d\overline{z}, \qquad \text{in } [z_0, \overline{H}] \tag{3b}$$

where $\overline{K} = \overline{z}(\overline{z} - \overline{\zeta})^2$ is the normalized eddy viscosity/diffusivity, $\overline{z} = zL^{-1}$, $\overline{u} = uU^{-1}$, $\overline{b} = bB^{-1}$, with boundary conditions $\overline{u}(z_0) = 0$, $\overline{u}(\overline{H}) = 0$, $\overline{b}(z_0) = \pm 1$ and $\overline{b}(\overline{H}) = 0$. Overbars $\overline{(\cdot)}$ will be omitted hereafter. Further, we introduce the following variable

$$f = b + iu, \tag{4}$$

and upon substitution of Eqs. 3a and 3b into Eq. 4, the system results into a complex ordinary differential equation (ODE) for the canonical variable f:

$$i \cdot f = d(K df/dz)/dz \qquad \text{in } [z_0, H], \tag{5}$$

with boundary conditions $f(z_0) = \pm 1$ and $f(H) = 0$. This technique for the decoupling of the system of Eqs. 3a and 3b is based on an ad hoc diagonalization. To solve Eq. 5 we first rewrite the equation in canonical form:

$$f'' + Pf' + Qf = 0, \tag{6}$$

where $(\cdot)' = \frac{\partial(\cdot)}{\partial z}$, $P(z) = (K)'/K$ and $Q(z) = 1/(iK)$. Second, it is an easy computation to show that rewriting Eq. 6 for $y = \frac{z}{\zeta}$ results in

$$f'' + \widetilde{P}f' + \widetilde{Q}f = 0, \tag{7}$$

where $(\cdot)' = \frac{\partial(\cdot)}{\partial y}$, $\widetilde{P}(y) = \gamma'(y)/\gamma(y)$ and $\widetilde{Q}(y) = 1/(i \cdot \zeta\gamma(y))$, with $\gamma(y) = y(y-1)^2$. Eq. 7 is a second order ODE with three regular singular points at $y = 0, 1$ and ∞, as in Morse and Feshbach (1953). This special case is known as the *equation of Papperitz* and its general solution is:

$$f(y) = \alpha(1-y)^{\mu}\, {}_2F_1(\mu, 1-\mu', 1+\mu-\mu', 1-y) + \beta(1-y)^{\mu'}\, {}_2F_1(\mu', 1-\mu, 1+\mu'-\mu, 1-y), \tag{8}$$

where ${}_2F_1$ are *Gaussian hypergeometric functions* and μ, μ' are the solutions to the degree two equation

$$x^2 + x + 1/(i\zeta) = 0.$$

Note that the general solution to Eq. 7 is also often written using the *Riemann symbol*:

$$\left\{ \begin{array}{cccc} 0 & 1 & \infty & \\ \lambda & \mu & \nu & y \\ \lambda' & \mu' & \nu' & \end{array} \right\}$$

where, in this case, μ and μ' are as above, $\lambda = \lambda' = 0$ and $\nu = 0$, $\nu' = 2$. Upon back-substitution of the independent variable and specification of the integration constants α and β (through the imposition of boundary conditions), the solution in terms of u and b is derived by separating the real and imaginary part of f

$$u(z) = \mathrm{Re}(f(z)), \qquad b(z) = \mathrm{Im}(f(z)). \tag{9}$$

3 Specification of of K(z)

The model assumes $Pr = 1$, i.e. $K_M = K_H = K$, although in reality they are slightly different. This assumption is justified based on the degree of accuracy of the considered study. Further, as stated in the preceeding section, we assume eddy diffusivities in line with the classic O'Brien's type (O'Brien, 1970), viz. $K = Az(z-\zeta)^2$, where A is a prefactor and $\zeta > H$ controls both shape and magnitude of K. The O'Brien model has often been used in studies of stable boundary layers, see for instance Pielke (1984) and Stull (1988), and a generalized O'Brien model was also recently adopted in Grisogono and Oerlemans (2001) to study slope flows. The properties of $K(z)$ in slope flows were thorougly justified in Grisogono and Oerlemans (2002); we here recall the main criteria that $K(z)$ should honor:

1. realizability condition: $K(z) \geq 0$;
2. $K(z << \infty) = 0$;
3. $\max(K(z))$, reached at $z = h$, must lie within the dynamic and thermal boundary layers;

4. $h > \max(2z_j, z_{inv})$;

where z_j is the height of the LLJ, and z_{inv} is the height of the surface inversion layer (in general we have $z_{inv} > z_j$). In addition, assuming Monin-Obukhov similarity theory to hold for the near wall regions (which is itself a subject of debate), one would ideally specify $K(z)$ in order to satisfy:

$$K(z) = \kappa u_* z \qquad z \in [z_0, z_s], \tag{10a}$$

$$K(z) = f(u_*, z) \mid d^2 f/dz^2 < 0 \qquad z \in (z_s, H], \tag{10b}$$

where z_s is the upper boundary of the constant-flux layer, κ is the Von Kármán constant, and $u_* = \kappa z (du/dz)|_{z_0}$, is the so-called friction velocity. Based on recent direct (DNS) and large-eddy simulation (LES) results (not shown) we make the additional assumption that h is located in the neighborhood of the first zero of the u velocity profile, well above z_j but within the dynamic and thermal boundary layers (under such constraint h identifies the lower boundary of the return flow). We will show hereafter that the solution is poorly sensitive on the exact value of h, as long as the resulting domain height $H < \zeta$ is large enough to accomodate the dynamic and thermal boundary layers. Knowledge of $dK/dz|_{z=z_0}$ and h allows to univocally specify $K(z) = Az(z-\zeta)^2$. A possible alternative would be to specify $dK/dz|_{z=z_0}$ and $\max(K)$. The size of the integration interval should be chosen as large as possible, under the constraint $H < \zeta$. Throughout the study we will set $H = \zeta - \zeta/100$, which allows to fully represent the dynamic and thermal boundary layers over a broad range of z_0 values. Note that in general it is not possible to satisfy Eqs. 10a directly, since the specification of K has to be done a-priori, and u_* depends on the solution. The chosen normalization allows to overcome this limitation, and highlights the linear dependence of the length scales of the flow on u_* ($A \propto u_* \propto L$). One could therefore first solve for $\overline{u}$ and $\overline{b}$, and then re-dimensionalize the problem, imposing $A = \kappa u_*/\zeta^2$ thus resulting in $K(z) = \kappa u_* z$, in agreement with Eq. 10a.

Despite the restrictive form of the model parameter $K(z)$, the formulation allows for exact integration of Eqs. 1 and 2, thus providing a useful reference to test approximate solutions such as the WKB (Grisogono and Oerlemans, 2001) and the dependence of the flow on the additional model parameter z_0. Further, the formulation can be used to validate numerical solutions of the Prandtl model equations (Eqs. 1 and 2).

4 Examples

In Fig. 1 we compare the new analytic solution (A1 in the following) against the constant-K (A2), the WKB (A3) and a numerical solution (N1), for a chosen z_0, ζ. ζ is specified so that h is located at the first zero of the $u(z)$ profile. The constant-K value is fixed to $K^+_{\mathrm{A2}} = \max(K^+_{\mathrm{A1}})/3$. Profiles for N1 are derived as direct numerical solution the system of ODEs defined by Eqs. 3a and 3b, where a second-order accurate centered finite difference discretization is adopted with

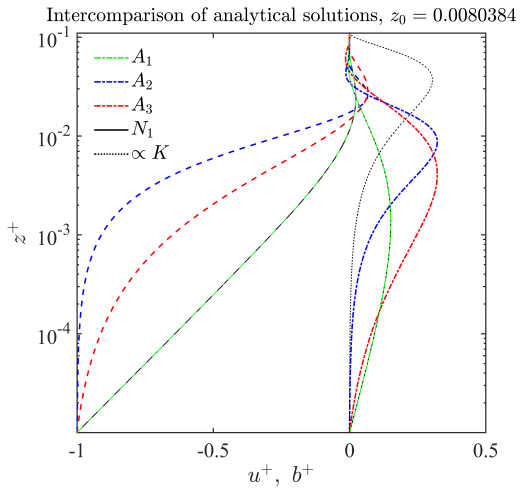

Fig. 1 Comparison of the new analytic solution (A1) against the constant-K (A2), the WKB (A3) and a numerical $1D$ solution (N1). Analytic profiles of normalized velocity ($\overline{u}$) are denoted with dot-dashed lines whereas analytic profiles of normalized buoyancy ($\overline{b}$) are denoted by dashed lines. Here $\overline{z}_0 = 0.00001$ and $\overline{\zeta} = 0.1$. A corresponding dimensional profile is characterized by $\max(K) = 0.1$ m^{2}s^{-1} and $K(z = 0) = 10^{-5}$ m^{2}s^{-1}, in agreement with common atmospheric values.

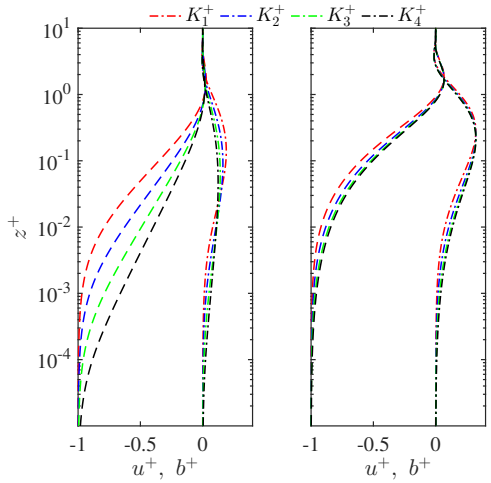

Fig. 2 Sensitivity of A1 (left) and A3 (right) profiles to variations in the diffusivity coefficient K^+. Normalized velocity values (u^+) are denoted with dot-dashed lines whereas normalized buoyancy values (b^+) with dashed lines. Equations are integrated in the interval $z^+ \in [0, 10]$, which is fully shown in the plot. Here we considered $A^+ = 6.75 \times 10^{-4}$ and $\epsilon^+ = (7.4, 1.5, 0.30, 0.06) \times 10^{-3}$. Under the constraint $K(z = 0) = 10^{-5}$ m^{2}s^{-1}, the corresponding set of dimensional kynematic diffusivities satisfy $\max(K) = 0.002, 0.01, 0.05, 0.25$ m^{2}s^{-1}.

Table 1 Set of parameters for re-normalization of the reference solution. The reference normalized solution is computed adopting $H^+ = 10, A^+ = 6.75 \times 10^{-4}, \epsilon^+ = 1.5 \times 10^{-3}$.

Value	Ref.	$\alpha 1$	α_2	N_1	N_2	$b_{s,1}$	$b_{s,2}$
α (deg)	30	15	60	30	30	30	30
N (Hz)	0.01	0.01	0.01	0.005	0.02	0.01	0.01
b_s (ms^{-2})	0.30	0.30	0.30	0.30	0.30	0.15	0.60

over $40,000$ collocation points and stretching the grid via a quadratic coordinate transform (at such resolution profiles are invariant to further refinements down to machine precision). The excellent match between A1 and N1 certifies the quality of results for both methods. A1 shows a remarkably strong inversion in the near surface regions ($z^+ < 1$), when compared against its analytical counterparts, suggesting an overdiffusive behaviour of both A2 and A3. For instance, normalized surface buoyancy gradients of simulation A1 are over an order of magnitude larger than those of A2 ($(db/dz)^+_{\mathrm{A1}}/(db/dz)^+_{\mathrm{A2}} = \mathcal{O}(10)$ as $z^+ \to 0$). Despite this, we observe a relatively good match between u^+_{A1} and u^+_{A3} in the interval $z^+ \in [0, 1]$, which confirms the enhanced dissipative properties of the A3 solution, when compared against the constant-K approach. To understand the importance of a decreasing eddy viscosity in the near surface regions, it is worth noting that $(du/dz)^+_{\mathrm{A1}}/(du/dz)^+_{\mathrm{A2}} = \mathcal{O}(10)$, whereas $(du/dz)^+_{\mathrm{A1}}/(du/dz)^+_{\mathrm{A3}} = \mathcal{O}(1)$ as $z^+ \to 0$. Overall the new solution exhibits significant variations when compared against A2 and A3, in both amplitude and location of maxima-minima. For instance, both the low-level jet height and the peak normalized velocity are significantly reduced, features that are of great importance for an accurate representation of the stable boundary layer and from a parameterization perspective (Mahrt, 1998). Further, from Fig. 2, it is clear that $\max(u^+_{\mathrm{A1}})$ now depends on the diffusive properties of the flow, i.e. $\max(u^+_{\mathrm{A1}}) = f(K^+)$, in constrast to its analytic counterparts, which predict $\max(u^+_{\mathrm{A2}}) = \max(u^+_{\mathrm{A3}}) = \sqrt{2}/2[(e^{(\pi/4)})/\sqrt{Pr}] = 0.32$, regardless of K^+. u^+_{A1} and b^+_{A1} also show a stronger dependence on the $K+$ parameter with respect to A3 profiles, in particular in the $z^+ \in [0, 1]$ interval. Overall, A1 predicts significantly reduced mass and buoyancy (horizontal) fluxes, viz. $\int_0^{H^+} u^+ dz^+, \int_0^{H^+} b^+ dz^+$, with respect to A3. To get acquainted with the proposed normalization Fig. 3 proposes a set of re-dimensionalized velocity profiles u (ms^{-1}) from a reference normalized solution. We propose a reference dimensional solution, characterized by $\alpha = 30$ deg, $N = 0.01$ Hz and $b_s = 0.3$ ms^{-2}, and consider variations in both sloping angle α, imposed buoyancy frequency N and imposed surface buoyancy b_s (see Table 1). Variations in the sloping angle α result in a modification of the normalization constant $L \propto \sin^{-1/2}$ which acts as a stretching of the independent variable z (no effects on $\max(u)$). In particular, the steeper the angle, the smaller the characteristic scales of the flow will become. Variations in the background stratification, viz. N, will modify both $L \propto N^{-1/2}$ and $U \propto N^{-1}$, yielding changes in the system, whose lengths and velocities will tend to decrease (increase) with increasing (decreasing) N. Further, variations in the prescribed surface buoyancy b_s will

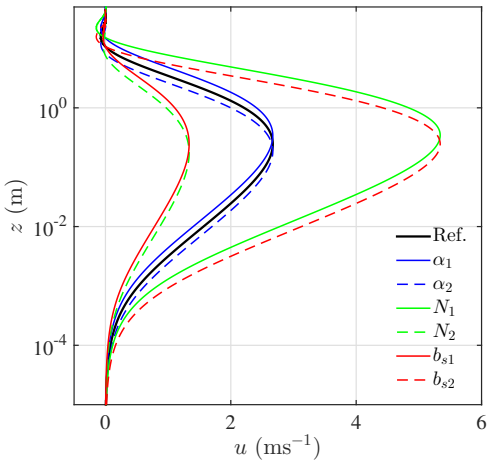

Fig. 3 Family of dimensional velocity profiles derived from re-dimensionalization of a reference normalized solution. The normalized solution is obtained in $z^+ \in [0, 10]$ for $A^+ = 6.75 \times 10^{-4}$ and $\epsilon^+ = 1.5 \times 10^{-3}$ (assuming $K(z = 0) = 10^{-5}$ m^{2}s^{-1}, the corresponding dimensional kynematic diffusivities satisfy $\max(K) = 0.01$ m^{2}s^{-1}). The considered set of parameters are reported in Table 1. Decreasing values of the parameters (with respect to the reference ones) are denoted with solid lines, increasing values by dashed lines.

scale both buoyancy and velocity profiles accordingly, since $b(z) \propto b_s$ and $u(z) \propto b_s$. As in both the classic Prandtl and WKB linear models, K^+ needs to be assigned a-priori; it is not coupled and does not feed back into the solution, which represents the main weakness of such linear approaches (Grisogono and Oerlemans, 2001).

5 Conclusions

We have derived a closed-form analytic solution of the Prandtl model equations, based on an ad hoc decoupling of the system and specific choice of the model parameter, resulting in a set of *equations of Papperitz*, characterized by three regular singular points. The new solution is valid for O'Brien-type eddy diffusivities (cubic polynomials) and Prandtl number of unity. For the considered settings the new solution represents an improvement with respect to both the classic constant-K and the more recent WKB solutions. New profiles show significant variations in both phase and amplitude of minima-maxima, stronger surface gradients are combined with overall reduced horizontal fluxes and the LLJ is further displaced toward the wall. The new solution suggests a somewhat different coupling between velocity and buoyancy – when compared against its analytical counterparts, showing a diffusivity dependent peak velocity and a remarkably strong inversion layer in the near surface location. In addition to a theoretical insight, the proposed solution can be used to improve

future stable boundary layer parameterizations when coupled with other parts of the boundary layer physics.

6 Acknowledgements

This research was primarily funded by the Swiss National Science Foundation (SNSF-200021-134892) and by the Competence Center for Environmental Sustainability (CCES-SwissEx) of the ETH domain. We are also grateful for funding from the NSERC Discovery Grant program.

References

Bender CM, Orszag SA (1999) Advanced Mathematical Methods for Scientists and Engineers I. Springer New York, New York, NY, DOI 10.1007/978-1-4757-3069-2, URL http://eprints.ucl.ac.uk/70187/http://link.springer.com/10.1007/978-1-4757-3069-2

Chu PC (1987) An instability theory of ice-air interaction for the formation of ice edge bands. Journal of Geophysical Research 92(7):6966, DOI 10.1029/JC092iC07p06966

Egger J (1985) Slope Winds and the Axisymmetric Circulation over Antarctica. Journal of the Atmospheric Sciences 42:1859–1867, DOI 10.1175/1520-0469(1985)042⟨1859:SWATAC⟩2.0.CO;2

Fedorovich E, Shapiro A (2009a) Structure of numerically simulated katabatic and anabatic flows along steep slopes. Acta Geophysica 57(4):981–1010, DOI 10.2478/s11600-009-0027-4, URL http://www.springerlink.com/index/10.2478/s11600-009-0027-4

Fedorovich E, Shapiro A (2009b) Turbulent natural convection along a vertical plate immersed in a stably stratified fluid. Journal of Fluid Mechanics 636:41, DOI 10.1017/S0022112009007757

Grisogono B, Oerlemans J (2001) Katabatic Flow: Analytic Solution for Gradually Varying Eddy Diffusivities. Journal of the Atmospheric Sciences 58(21):3349–3354, DOI http://dx.doi.org/10.1175/1520-0469(2001)058⟨3349:KFASFG⟩2.0.CO;2

Grisogono B, Oerlemans J (2002) Justifying the WKB approximation in pure katabatic flows. Tellus, A 54(5):453–462, DOI 10.1034/j.1600-0870.2002.201399.x

Gutman LN (1983) On the theory of the katabatic slope wind. Tellus, A 35(3):332–335, DOI 10.3402/tellusa.v35i3.11434

Gutman LN, Malbakhov VM (1964) On the Theory of the Katabatic Winds of Antarctica. University of Melbourne, Meteorology Department

Lykosov VN, Gutman LN (1972) Turbulent boundary layer above a sloping inderlying surface. Proceedings of the USSR Academy of Sciences 8:799–809, URL papers2://publication/uuid/B2EC0692-4251-4224-8185-A1AE8D9B00E9

Mahrt L (1998) Stratified Atmospheric Boundary Layers and Breakdown of Models. In: Theoretical and Computational Fluid Dynamics, vol 11, pp 263–279, DOI 10.1007/s001620050093, URL http://link.springer.com/10.1007/s001620050093

Monti P, Fernando HJS, Princevac M, Chan WC, Kowalewski TA, Pardyjak ER (2002) Observations of Flow and Turbulence in the Nocturnal Boundary Layer over a Slope. Journal of the Atmospheric Sciences 59:2513–2534, DOI 10.1175/1520-0469(2002)059⟨2513:OOFATI⟩2.0.CO;2

Morse PM, Feshbach H (1953) Methods of Theoretical Physics. McGraw-Hill

Nadeau DF, Pardyjak ER, Higgins CW, Parlange MB (2013) Similarity Scaling Over a Steep Alpine Slope. Boundary-Layer Meteorology 147(3):401–419, DOI 10.1007/s10546-012-9787-5, URL http://link.springer.com/10.1007/s10546-012-9787-5

Nappo CJ, Shankar RK (1987) A model study of pure katabatic flows. Tellus A 39(1):61–71, DOI 10.3402/tellusa.v39i1.11740, URL http://onlinelibrary.wiley.com/doi/10.1111/j.1600-0870.1987.tb00289.x/abstract

Nylen TH, Andrew G F, Doran PT (2004) Climatology of katabatic winds in the McMurdo dry valleys, southern Victoria Land, Antarctica. Journal of Geophysical Research 109:1–9, DOI 10.1029/2003JD003937

O'Brien JJ (1970) A Note on the Vertical Structure of the Eddy Exchange Coefficient in the Planetary Boundary Layer. Journal of the Atmospheric Sciences 27:1213–1215, DOI 10.1175/1520-0469(1970)027⟨1213:ANOTVS⟩2.0.CO;2, URL http://dx.doi.org/10.1175/1520-0469(1970)027<1213:ANOTVS>2.0.CO;2

Oerlemans J (1998) The atmospheric boundary layer over melting glaciers. In: Clear and Cloudy Boundary Layers, vol 48, Royal Netherlands Academy of Arts and Sciences, pp 129–153, URL http://igitur-archive.library.uu.nl/phys/2007-0716-203217/oerlemans{_}07{_}atmosphericboundarylayer.pdf

Oerlemans J, Vugts HF (1993) A Meteorological Experiment in the Melting Zone of the Greenland Ice Sheet. Bulletin of the American Meteorological Society 74(3):355–365, DOI 10.1175/1520-0477(1993)074⟨0355:AMEITM⟩2.0.CO;2

Oldroyd HJ, Katul G, Pardyjak ER, Parlange MB (2014) Momentum balance of katabatic flow on steep slopes covered with short vegetation. Geophysical Research Letters 41:4761–4768, DOI 10.1002/2014GL060313

Parish TR (1992) On the Role of Antarctic Katabatic Winds in Forcing Large-Scale Tropospheric Motions. Journal of the Atmospheric Sciences 49:1374–1385, DOI 10.1175/1520-0469(1992)049⟨1374:OTROAK⟩2.0.CO;2

Parish TR, Bromwich DH (1998) A Case Study of Antarctic Katabatic Wind Interaction with Large-Scale Forcing. Monthly Weather Review 126:199–209, DOI 10.1175/1520-0493(1998)126⟨0199:ACSOAK⟩2.0.CO;2

Pielke RA (1984) Mesoscale numerical modeling. Advances in Geophysics 23:185–344

Prandtl L (1942) Führer durch die Strömungslehre. Vieweg & Sohn, Braunschweig

Shapiro A, Fedorovich E (2007) Katabatic flow along a differentially cooled sloping surface. Journal of Fluid Mechanics 571:149, DOI 10.1017/S0022112006003302, URL http://www.journals.cambridge.org/abstract{_}S0022112006003302

Spalart P, Strelets M, Garbaruk A (2011) Quality and Reliability of Large-Eddy Simulations II. In: Evaluating Subgrid-ScaleModels for Large-Eddy Simulation of Turbulent Katabatic Flow, vol 16, pp 253–267, DOI 10.1007/978-94-007-0231-8, URL http://www.springerlink.com/index/10.1007/978-94-007-0231-8

Stull RB (1988) An Introduction to Boundary Layer Meteorology, vol 13. Springer, DOI 10.1007/978-94-009-3027-8, URL http://books.google.com/books?hl=en{&}lr={&}id=BK8P9rl-CB4C{&}oi=fnd{&}pg=PR11{&}dq=AN+INTRODUCTION+TO+BOUNDARY+LAYER+METEOROLOGY{&}ots=ocdv6uHfgM{&}sig={_}vkNpJ4pNjW906TJ849rGw8vOCM